This article has been accepted for publication in a future issue of this journal, but has not been fully edited. Content may change prior to final publication. Citation information: DOI 10.1109/TAP.2018.2836463, IEEE Transactions on Antennas and Propagation

A Compact Wideband Flexible Implantable Slot Antenna Design With Enhanced Gain

Soumyadeep Das, *Student Member, IEEE*, and Debasis Mitra, *Member, IEEE*

***Abstract*- In this communication, a CPW-fed, compact, wideband dual-ring slot antenna for biomedical applications in ISM frequency band is presented. This implantable antenna is designed using thin and biocompatible substrate-superstrate layers to achieve human body insulation as well as flexibility. Despite showing good antenna performances, only the realized gain value is observed to be reduced (-12 dB). To improve the antenna gain, a metamaterial (MTM) array with epsilon very large (EVL) behavior has been introduced on the superstrate of the implantable antenna. Using the MTM, about 3 dB gain enhancement has been observed. Even after the introduction of the metamaterial superstrate, wideband characteristic and flexibility are maintained. Also, the SAR analysis of the antenna configuration with and without MTM has been studied. A low SAR is obtained in both the cases. The fabricated antenna parameters have been measured with the in-vitro test by immersing the antenna inside single layer tissue emulating gel, as well as, inside a chicken breast slab.**

***Index terms*- Implantable Antenna, Flexible, Wideband, Compact, Biomedical application, Gain enhancement.**

I. Introduction

Basic requirements for designing a biomedical implantable antenna are compact size, larger bandwidth, flexibility and low specific absorption rate (SAR). To ensure proper placement of the implantable antenna inside the human torso, the overall size of the antenna should be reasonably small. Recently, different techniques in antenna miniaturization for the sake of implantable antenna have been developed by various research groups [1-5]. A significant size reduction has been achieved by increasing the current path with embedded meandered slot and open slots in the ground plane [1] and multiple slots over the patch [2]. For a better level of miniaturization, a periodic structure has been used in the substrate of an implantable antenna [3]. Afterwards, a split ring resonator (SRR) [4], and a combination of Complimentary SRR and C-shaped slot [5] has been effectively used to reduce the antenna size. Though the above techniques result in high amounts of size reduction, the design complexities of the antennas are not desirable for biomedical implantable applications.

Larger Bandwidth is another demand for implantable antenna design to provide the required mobility to the dynamic implantable antenna [6]. In general, bandwidth enhancement has been achieved by merging two resonating frequency modes. To obtain larger bandwidth in [7], two π-shaped meandered strips are utilized on the Planar Inverted F antenna (PIFA). In [8], a C-shaped ground is coupled with sigma shaped monopole radiator to achieve wide bandwidth by enabling an additional resonant mode. Although the techniques are advantageous, their applications would be limited by design constraints, as the design becomes bulky and complicated.

Another important design aspect of an implantable antenna is flexibility. A flexible antenna can be used as a part of the flexible electronic circuit, which can be implanted inside the human torso [9]. Also, the flexible nature prevents the antenna from any damage due to the unpredictable movement of muscle or tissue. A flexible slot dipole antenna, covered with a coating of biocompatible material Polydimethylsiloxane (PDMS), has been reported in [10]. Antenna structure, presented in [8], has been further modified with thin layer of a substrate to achieve flexibility in [11]. It is noticed that, in general, the SAR value increases for the flexible implantable antennas.

In this communication, we present a compact and flexible circular ring slot antenna with wideband characteristics. This circularly shaped antenna with two concentric ring slots makes the configuration simple and compact in size. This dual ring topology excites two nearly spaced resonant frequencies, to obtain larger bandwidth. The implantable antenna is designed with thin layers of biocompatible substrate and superstrate to make the antenna flexible. A significantly low SAR has also been obtained in this case. However, it is observed that the implantable antenna gain has been reduced may be due to absorbing nature of the human tissue.

In order to improve the antenna gain, an efficient gain enhancement technique has been used for the implantable slot antenna. In the previous literatures, different techniques were proposed for implantable antenna gain enhancement. Recently, the implantable antenna gain has been increased by introducing external structures, such as printed grid surface [12] or the combination of parasitic ring and hemispherical glass lens [13]. Due to the inclusion of these external structures, the above-mentioned approaches restrict the entire antenna system to be implanted inside patient's body. Hence, some alternative techniques must have been used for the gain enhancement of implantable antennas. To serve this purpose, inclusion of metamaterial structures are aimed at, as they are already being used extensively for free space antenna gain enhancement. The grounded metamaterial, proposed by Lovat et al. in [14], is used for high gain/ directivity with a compact antenna configuration [15], [16], and [17] for free space antennas.

In the current work, the grounded metamaterial technique [14], has been used for the gain enhancement of the proposed implantable ring-slot antenna. In this regard, a 2 × 2 array of metamaterial unit cell with Epsilon Very Large (EVL) property has been designed on the superstrate layer. At the operating frequency of 2.45 GHz, about 3 dB gain improvement is observed for the implantable slot antenna, sustaining its compact and flexible nature. Even after the inclusion of the metamaterial array, the wideband characteristic of the implantable slot antenna remains unaffected. Also, the SAR value remains less than other implantable antennas in the literature. This metamaterial loaded implantable slot antenna has been validated inside the human tissue mimicking gel and as well as a chicken tissue sample. Also, the performances of the enhanced gain implantable antenna are compared with the other recently published biomedical implantable antennas.

II. Implantable Slot Antena Design & Performance Analysis

This article has been accepted for publication in a future issue of this journal, but has not been fully edited. Content may change prior to final publication. Citation information: DOI 10.1109/TAP.2018.2836463, IEEE Transactions on Antennas and Propagation

In this section the design and analysis of a compact, wideband and flexible implantable slot antenna has been discussed. The antenna has been simulated inside a single as well as multilayer human tissue model.

A. Antenna Geometry & Analysis

The implantable slot antenna configuration consists of two concentric rings of equal slot width d, is shown in Fig. 1(a). These ring slots with the outer radius R_1 and R_2 respectively, are fabricated on a 10 mm × 10 mm Kapton polyimide substrate with dielectric constant (ε_r) 2.91 and loss tangent 0.005. A superstrate layer of Rogers 6010 having high dielectric constant 10.2 and loss tangent 0.0023 is placed over the antenna. High dielectric value of the superstrate material decouples the antenna from the absorbing, lossy surrounding as well as stabilizes the effective permittivity fluctuations around the antenna [18]. Both these substrate and superstrate materials are chosen based on impedance matching, minimum reflection and biocompatibility. To achieve flexibility, both superstrate and substrate thicknesses (h) are used as 0.2 mm. Hence, the total dimension of the proposed antenna is 10 mm × 10 mm × 0.4 mm. Here, Co-Planar Waveguide (CPW) feed is used for 50 Ω impedance matching by using appropriate trace width (W) and ground plane spacing (S). Fig. 1(b) shows the placement of the proposed antenna inside a single layer human-muscle model. Table I shows all the design parameters of the implantable slot antenna.

TABLE I
Design parameters (in mm) of the implantable slot antennas

L	S	W	R_1	R_2	h	D
10	0.85	1	3.5	2.5	0.2	0.5

Ansys High Frequency Structural Simulator (HFSS) has been used for the antenna design and analysis. A multi-layered human arm model is designed and the antenna is analyzed by placing it inside muscle layer. Fig. 1 (c) and (d) refer to the cylindrical human arm model and the placement of the antenna inside the model, respectively. The dielectric properties of the various layers of the multi-layer arm model are listed in Table II. For simplicity, the proposed antenna is analyzed in the single layer tissue model as well. The design of the antenna is primarily governed by the equation, $f_r = c/\lambda_g\sqrt{\varepsilon_{eff}} \approx c/l_r\sqrt{\frac{\varepsilon_r+1}{2}}$, here, λ_g is the guided wavelength, ε_{eff} is the effective permittivity, f_r is the resonating frequency of the antenna, l_r is the perimeter of the ring, ε_r denotes the relative dielectric constant of substrate, superstrate combined. The effect of the high dielectric constant of the biomedical environment also affects the effective dielectric constant. While considering only the single ring, i.e., the outer ring, a single resonance is found at around 2.9 GHz. Due to the insertion of the inner ring two different frequency modes are generated. The combining effect of those two nearly placed frequency bands provides a wideband characteristic of the proposed antenna.

An equivalent circuit model of the implantable slot antenna has been designed using ADS software which is given in Fig. 2 (a). The coupling elements are inserted in the circuit diagram to model the interaction between the individual slot sections and the CPW feed extension with the CPW feed line. The capacitance C_f is being used for the feed section, whereas, the LC coupling circuit having L_1 and C_1 models the interaction

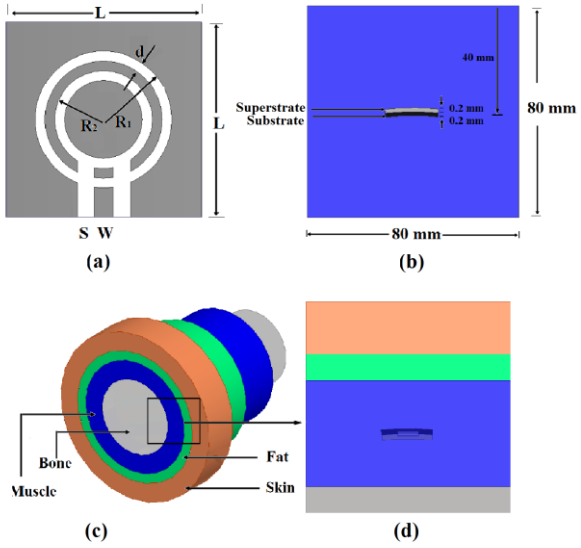

Figure 1. Implantable slot antenna geometry: (a) Top view of the antenna, (b) Antenna Placed at the center of a cubic single layer human-muscle model, (c) 4-layer cylindrical human arm model, (d) A selected cubic cross section of the model with the antenna placed inside muscle layer.

TABLE II
Dielectric properties of various human tissues
in an operating frequency of 2.40GHz [19]

Tissue Type	Skin	Fat	Muscle	Bone
Dielectric Constant (ε_r)	42.92	5.285	52.79	11.41
Bulk Conductivity [σ (S/m)]	1.562	0.102	1.705	0.385

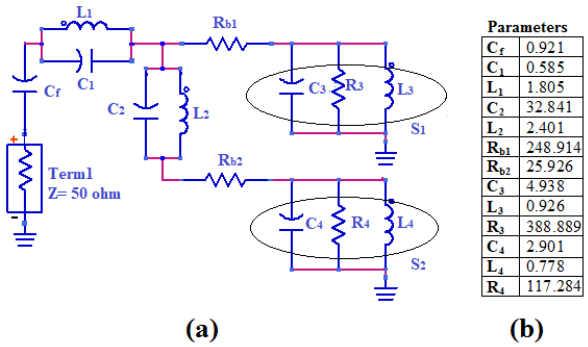

Figure 2. Equivalent circuit model for the implantable slot antenna; (a) circuit diagram, (b) corresponding lumped elements values. All the values of C in pF; L in nH; and R in ohm.

between the feed extension and the CPW line. This feed line directly excites the outer ring and couples the inner ring with another coupling LC circuit having inductor and capacitor L_2 and C_2, respectively. Now the sections marked as S_1 and S_2 correspond to two different resonating frequencies, which are generated due to dual-ring configuration of the antenna. It is observed that the first resonance is contributed by the outer ring slot, whereas, the second resonance is mainly due to the inner ring slot. Here, the resistances R_{b1} and R_{b2} indicate the loss due to the biomedical environment, inside which the proposed antenna has been analysed. The circuit parameters in the model, shown in Fig. 2 (b), have been extracted using ADS and matched with the simulated as well as measured return loss characteristics in Fig. 3(a).

B. Characteristics of Return Loss and Radiation Pattern

The dual ring slot antenna has been simulated inside both the single layer and multi-layer human tissue model. The simulated

This article has been accepted for publication in a future issue of this journal, but has not been fully edited. Content may change prior to final publication. Citation information: DOI 10.1109/TAP.2018.2836463, IEEE Transactions on Antennas and Propagation

and the measured results for the return loss characteristics are shown in Fig. 3 (a). A wideband characteristic is observed as two resonating frequency modes overlap with each other. This is well supported by the magnetic current distribution of the ring slots. The magnetic current distribution is simulated over the slot of the implantable antenna design for both the resonating frequencies. It can be observed from the Fig. 4, that the first resonating mode is essentially caused by the extension of the magnetic current path at the outer most ring slot, while, the second resonating mode is caused mainly due to the inner ring slot.

Radiation patterns, given in Fig. 3 (b) and (c), are almost omnidirectional, as required for an implantable antenna. At the operating frequency of 2.45 GHz, the realized antenna gain is approximately -12 dB and the calculated efficiency of the antenna is around 2.5%–5.6%. The reduced values of both gain and efficiency of the antenna are observed, which may be due to the absorbing nature of the biological tissue.

C. *Effects of Bending*

For analyzing the effect of bending, the flexible implantable slot antenna is folded with the radius of curvature R, which is shown in Fig 5 (a). The variation of R with antenna parameters has been represented in Fig. 5 (b)-(d). It is observed in Fig. 5 (b) that, there is no significant effect of bending on the antenna return loss. From the Fig. 5 (c) and (d), it is also noticed that, as R varies, the real and imaginary part of the impedance value stays around 50 ohms and 0 ohms respectively, near the operating frequency 2.45 GHz. Hence, a good amount of impedance matching has been observed for the flexible antenna configuration.

D. *Variation of Substrate Thickness*

The effect of the variation of the antenna substrate thickness has been shown in Fig. 6 (a) and (b). When the substrate thickness increases, as shown in Fig. 6 (a), the volume loss density of the antenna decreases while the surface loss density remains almost unchanged. As the thicknesses of substrate and superstrate are taken very low compared to the operating wavelength ($<0.01\lambda_0$) in a free space, loss due to surface wave can be ignored [11]. Subsequently, the antenna efficiency improves because the efficiency of an antenna depends on the power loss due to impedance mismatch, dielectric losses and surface wave.

The SAR is an important aspect of biomedical implantable antennas and it gives the measure of absorbed power within a unit mass of biological tissue. Slope discontinuities of magnetic vector potential may increase the SAR value [8]. Also, the slope of the vector potential dominates the near field of an antenna [11]. Hence, the near field of the antenna must govern the SAR characteristics and uniformity in current distribution may reduce the SAR value [11]. Fig. 6 (b) shows as the near E field decreases with the increase of substrate thickness, so as SAR value. Though we are aiming at low SAR value as a basic goal of the biomedical implantable antenna, we have to optimize the substrate thickness, so that both flexibility and the low SAR value can be achieved. For the implantable slot antenna with 0.2 mm substrate thickness, the average SAR value of 76 W/Kg over a 1g tissue model for 1 W input power has been observed when it is analysed inside a single layer model.

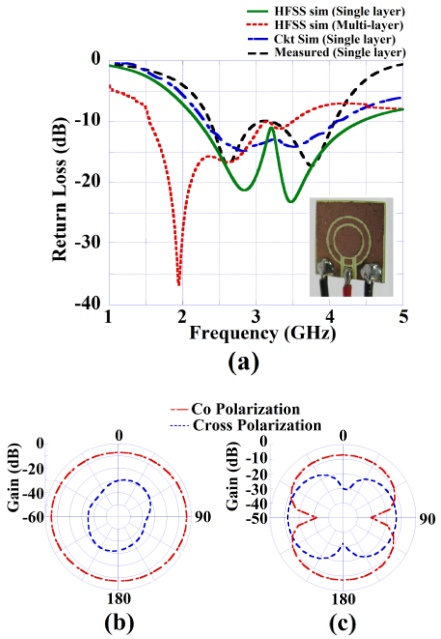

Figure 3. Implantable slot antenna characteristics: (a) Return loss characteristics of the antenna and the prototype antenna (inset); Radiation pattern at 2.45 GHz: (b) XZ plane, (c) YZ plane.

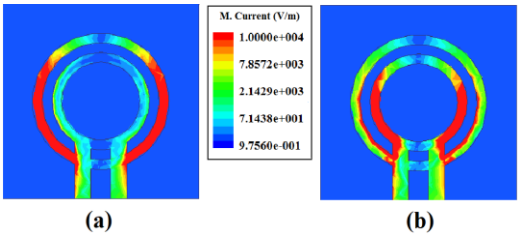

Figure 4. Magnetic current distribution for the dual ring slot antenna; (a) at the first resonating frequency, (b) at the second resonating frequency.

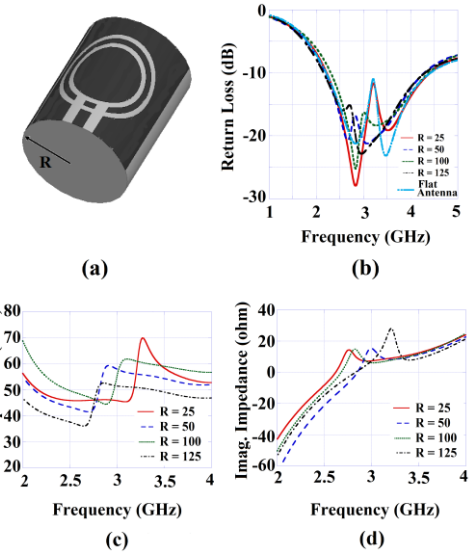

Figure 5. Effects of variations in the radius of curvature (R) for the implantable flexible slot antenna; (a) Curved configuration, (b) Return loss, (c) Real part of impedance, (d) Imaginary part of impedance.

E. *SAR distribution*

The SAR value should be within the range, set by the IEEE C95.1-1999 standard. For safety, the average SAR should be less than 1.6 W/Kg for a 1g- body model. SAR analysis has

This article has been accepted for publication in a future issue of this journal, but has not been fully edited. Content may change prior to final publication. Citation information: DOI 10.1109/TAP.2018.2836463, IEEE Transactions on Antennas and Propagation

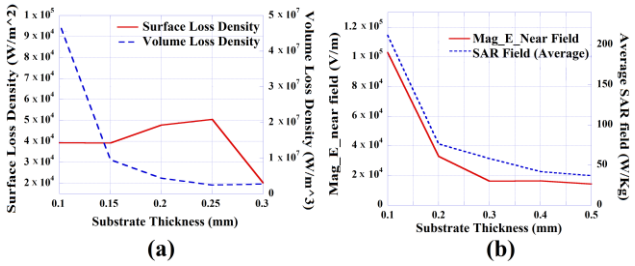

Figure 6. Effects of variations in the substrate thickness; (a)Surface and volume loss density of the proposed antenna, (b) SAR and near E-field magnitude variation of the proposed antenna.

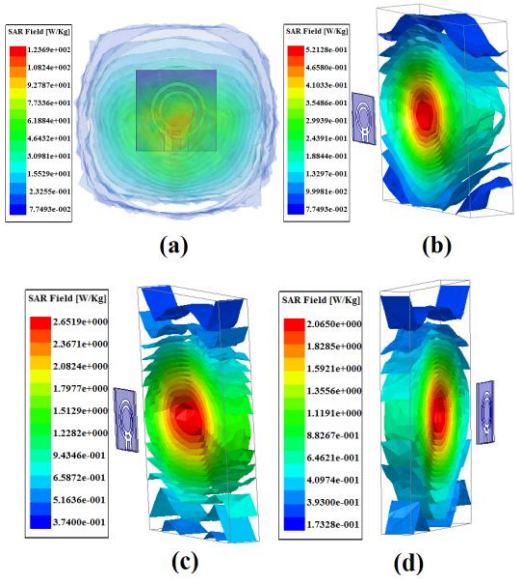

Figure 7. Average SAR analysis in (a) Muscle layer, (b) Skin Layer, (c) Fat Layer, (d) Bone layer, when the antenna is placed inside the muscle layer.

also been simulated inside the multi-layered tissue model by placing the antenna inside the muscle layer. The difference in dielectric properties of different layers and the placement of the antenna inside the multilayer model governs the average SAR distribution for each and every layer. Fig. 7 (a)-(d) present the SAR distribution in various tissue layers and the maximum average SAR over the multilayer tissue model is observed approximately 124 W/Kg for 1g model. This average SAR distribution shows that SAR is maximum in the muscle layer, where the antenna is placed and it decreases for other surrounding layers. This estimated SAR value is for 1 W input power. Hence, to keep the SAR value within specified limit, input power should be reduced to 7.2 mW.

III. Gain Enhancement of the Implantable Slot Antenna Using Metamaterial Structures

For the implantable slot antenna in the previous section, the reduced antenna gain is observed may be due to the absorbing nature of the human tissue. In the following section, a metamaterial based efficient technique is presented to enhance the gain of the proposed antenna.

As described by Lovat et al. in [14], grounded metamaterial superstrate with the mu very large (MVL) and epsilon very large (EVL) properties are required for improving the broadside gain and directivity of an electric dipole and magnetic dipole source respectively. Generally, the EVL characteristic has been observed in electrical-LC (ELC) type resonator unit cells. Smith et al. first introduce an ELC resonator structure in [20]. In our work, antenna and the MTM superstrate has been simulated inside a biomedical environment, which is anisotropic in nature. Hence the MTM unit cell characteristics, the effective medium parameters, such as effective permittivity (ε_{eff}) and permeability (μ_{eff}) have been extracted with an advanced retrieval method using Kramers-Kronig relationship [21]. Some required optimizations in dimensions have been performed to achieve the EVL characteristics of the metamaterial superstrate inside the human tissue environment at the operating frequency of 2.45 GHz, and it is shown in Fig. 8 (a). As it can be observed from Fig. 8 (b), that the real part of the effective permittivity of the metamaterial superstrate is high and it varies between 15 and 20 in the considered frequency range, with significantly low loss characteristics. Therefore, this MTM with EVL property can be used for enhancing the gain of an implantable slot antenna.

In this study, to improve the gain, a finite array of 2 × 2 unit cell is printed on the superstrate of the implantable slot antenna, which is shown in Fig. 8 (c). This metamaterial array configuration has been designed on the existing superstrate of the implantable biomedical antenna. As no additional dielectric slab is required for loading the metamaterial unit cell, this entire antenna configuration ensures a greater level of vertical compactness. This compact configuration is suitable for implanting into the human tissue. The simulated and measured return loss characteristics of the MTM loaded implantable slot antenna are given in Fig. 9 (a). It is observed that the resonant frequency of the implantable antenna is not affected much by the introduction of the metamaterial slab. Moreover, the antenna radiation patterns have also been analyzed, and are shown in Fig 9 (b), (c). By comparing the radiation patterns in Fig. 3 (b)-(c) and Fig 9 (b)-(c), it can be observed that the inclusion of MTM superstrate reduces the cross polarization for both XZ and YZ plane. Gain comparison between the implantable slot antenna and MTM loaded slot antenna is shown in Fig. 10 (a), (b) and (c). 3D polar plots for both the implantable antenna and the MTM loaded implantable antenna, shown in 10 (a) and (b) respectively, ensures the increase in gain after the MTM loading. Enhancement in antenna gain can be inferred as well from the gain vs frequency analysis represented in Fig. 10 (c). About 3 dB gain enhancement has been observed at the required operating frequency, indicated by the shaded zone in the figure.

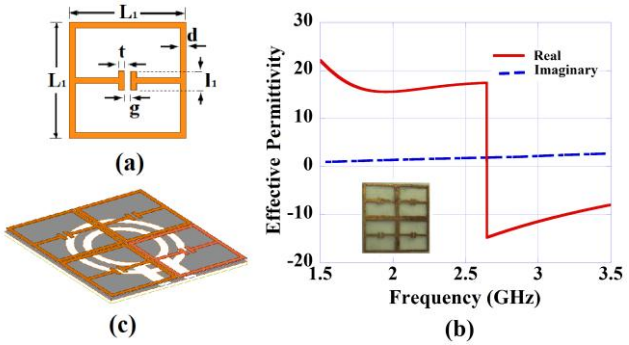

Figure 8. Metamaterial inclusion inside human tissue; (a) MTM unit cell, where dimensions are in mm: L_1=4.7, d=0.25, l_1=1, t=0.2, g=0.1, (b) Effective permittivity characteristic of the unit cell, (c) MTM loaded implantable slot antenna.

This article has been accepted for publication in a future issue of this journal, but has not been fully edited. Content may change prior to final publication. Citation information: DOI 10.1109/TAP.2018.2836463, IEEE Transactions on Antennas and Propagation

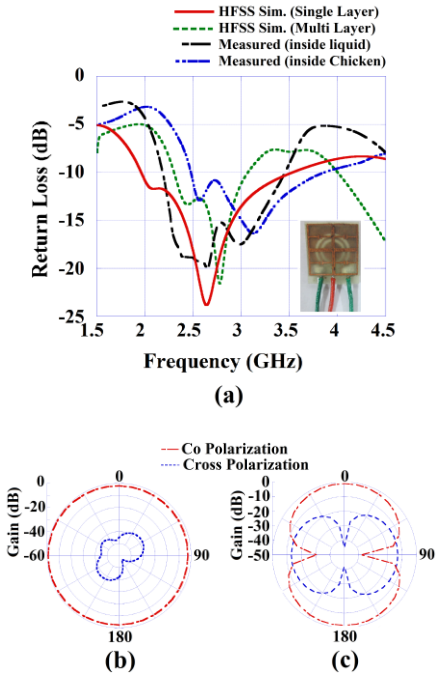

Figure 9. MTM loaded Implantable slot antenna characteristics; (a) Return loss characteristics of the antenna (simulated and measured) & prototype of the antenna (inset); Radiation pattern at 2.45 GHz: (b) XZ plane, (c) YZ plane.

SAR distributions in various tissue layers are analysed for the MTM loaded slot antenna and presented in Fig 11 (a)-(d). It can be observed that the maximum average SAR value is 131 W/Kg at the muscle layer, where the antenna is placed. Therefore, due to the inclusion of MTM unit cell, SAR value doesn't change significantly. The maximum SAR values and maximum allowable input power are shown in Table III for the dual ring slot antenna with and without MTM unit cell inside single layer and multilayer tissue model.

IV. Discussion & Measurement

In the previous section, a significant gain enhancement has been observed for the proposed wideband flexible implantable slot antenna. Even with the inclusion of the grounded metamaterial the required wideband characteristics has been retained, as shown in Fig. 9 (a). An impedance bandwidth of 57% can be observed from the figure. This proposed antenna has been compared with several recently reported implantable antennas operating in various biomedical frequency bands, such as MedRadio band and ISM bands, in Table IV. Here, the proposed antenna shows a higher realized gain of -9 dB and lower SAR value of 131 W/Kg for 1-g model. The rationale of validation and characterization has been described in this section with the measurement setup shown in Fig. 12 (a) and (b), with tissue mimicking gel and chicken breast slab, respectively. The Anritsu MS2025B network analyzer and 50Ω SMA connector probes are used for measuring the proposed implantable antenna parameters. As the antenna size is very small compared to the connector port, single core copper wire has been used to connect it with the feed line and the ground plane as well. This arrangement with copper wire is strictly for experimental purpose. For the in-vitro test the MTM loaded implantable antenna is immersed at a depth of 10 mm into the human tissue mimicking gel for analysis. This liquid shows a property nearly similar to a human muscle tissue of dielectric

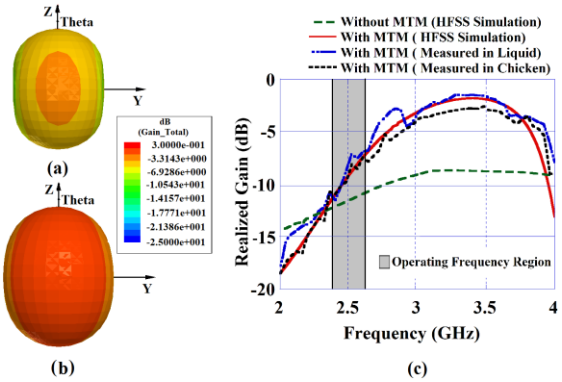

Figure 10. Gain Comparison for Implantable slot antenna and MTM loaded slot antenna; (a) 3D radiation pattern for implantable slot antenna, (b) 3D radiation pattern for implantable slot antenna with MTM, (c) realized gain plot over frequency.

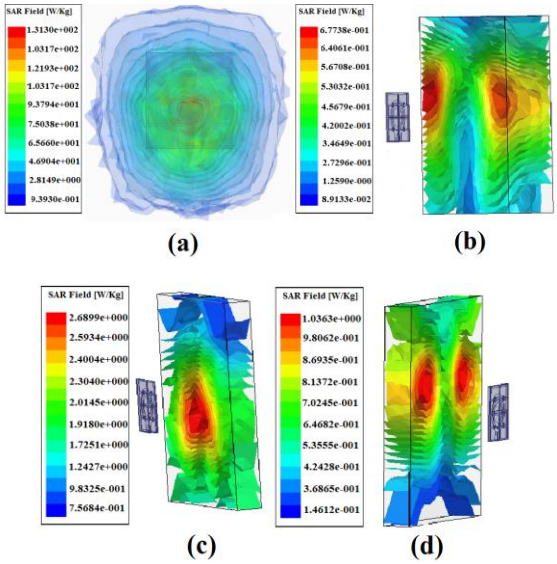

Figure 11. Average SAR analysis for antenna with MTM; (a) Muscle layer, (b) Skin Layer, (c) Fat Layer, (d) Bone layer, when the antenna is placed inside the muscle layer.

TABLE III
Maximum SAR (net input power = 1 w), and maximum allowable net-input power for the implantable slot antenna

Analysis Geometry	Type	Max SAR (W/Kg)	Max net-input power (mW)
Single Layer	Without MTM	76	7.2
	With MTM	297	5.6
Multi Layer	Without MTM	124	6.2
	With MTM	131	6.0

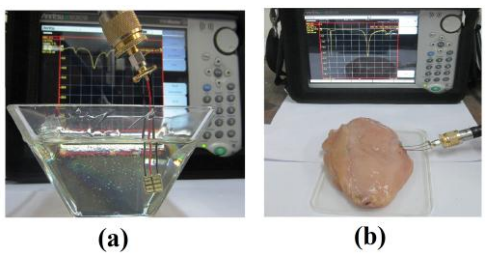

Figure 12. Measurement setup for the proposed implantable slot antenna; (a) inside tissue mimicking liquid, (b) inside chicken tissue.

constant (ε_r) = 52.79 and loss tangent (tan δ) =0.234. The test is also carried out by placing the antenna at 10 mm inside a chicken breast slab. At 2.45 GHz and 25^{0}C the dielectric

This article has been accepted for publication in a future issue of this journal, but has not been fully edited. Content may change prior to final publication. Citation information: DOI 10.1109/TAP.2018.2836463, IEEE Transactions on Antennas and Propagation

TABLE IV
Performance comparison with the recent reported implantable antennas

Ref.	Freq.	Size mm^3	BW/f_c %	Gain dBi	SAR W/Kg	Ant. Flexibility
[8]	450 MHz	$0.027\lambda_0 \times 0.027\lambda_0 \times 0.00213\lambda_0$	67.80	-27.8	161	No
[11]	450 MHz	$0.026\lambda_0 \times 0.026\lambda_0 \times 0.00027\lambda_0$	64.00	-32.0	230	Yes
[4]	402 MHz	$0.013\lambda_0 \times 0.016\lambda_0 \times 0.0017\lambda_0$	34.50	xx	905	No
	2.45 GHz	$0.082\lambda_0 \times 0.098\lambda_0 \times 0.01037\lambda_0$	58.70	-21.0	769	
[3]	400 MHz	$0.012\lambda_0 \times 0.013\lambda_0 \times 0.00187\lambda_0$	20.44	xx	296	No
	2.40 GHz	$0.072\lambda_0 \times 0.076\lambda_0 \times 0.0112\lambda_0$	36.73	xx	490	
[5]	2.45 GHz	$0.069\lambda_0 \times 0.069\lambda_0 \times 0.01037\lambda_0$	12.20	-17.0	xx	No
[22]	915MHz	$0.024\lambda_0 \times 0.018\lambda_0 \times 0.00152\lambda_0$	9.84	-28.5	971	No
	2.40GHz	$0.064\lambda_0 \times 0.048\lambda_0 \times 0.004\lambda_0$	8.57	-22.8	807	
[23]	4.80GHz	$0.08\lambda_0 \times 0.08\lambda_0 \times 0.0256\lambda_0$	14.80	-25.4	xx	No
our work	2.45 GHz	$0.082\lambda_0 \times 0.082\lambda_0 \times 0.00327\lambda_0$	57.00	-9.0	131	Yes

xx: Not given

constant (ε_r) and loss tangent (tan δ) are 55.2 and 0.349, respectively [24], which is very close to the properties of human muscle.

V. Conclusion

The design and analysis of a compact and flexible implantable slot antenna is addressed in this paper. The antenna shows wideband characteristics and low SAR values inside the absorbing biological medium with corresponding decrease in antenna gain and efficiency. Therefore, an antenna gain enhancement technique is discussed using MTM loaded superstrate. This technique ensures no additional dielectric structure is required and allows the pre-existing antenna superstrate to be used for metamaterial designing. Thus this technique makes the MTM loaded antenna configuration compact and fully implantable. It has also been observed that due to the inclusion of MTM superstrate, the SAR value of the antenna doesn't change significantly**.** A suitable implantable antenna in-vitro test-bed with both the human tissue emulating liquid and chicken breast slab is used for antenna validation.

Acknowledgment

For research support, S. Das acknowledges the Visvesvaraya Ph.D. scheme for Electronics & IT research fellowship award and D. Mitra acknowledges the Visvesvaraya Young Faculty research award, under MeitY, Govt. of India.

References

[1] C. Liu, Y.-X. Guo, and S. Xiao, "A hybrid patch/slot implantable antenna for biotelemetry devices," *IEEE Antennas and Wireless Propagation Letters*, vol. 11, pp. 1646-1649, 2012.

[2] R. Li and S. Xiao, "Compact slotted semi-circular antenna for implantable medical devices," *Electronics Letters*, vol. 50, no. 23, pp. 1675-1677, Nov. 2014.

[3] S. Hashemi and J. Rashed-Mohassel, "Miniaturization of dual band implantable antennas," *Microwave and Optical Technology Letters*, vol. 59, no. 1, pp. 36-40, Jan. 2017.

[4] H. Zhang, L. Li, C. Liu, Y.-X. Guo, and S. Wu, "Miniaturized implantable antenna integrated with split ring resonate rings for wireless power transfer and data telemetry," *Microwave and Optical Technology Letters*, vol. 59, no. 3, pp. 710-714, Mar. 2017.

[5] X. Y. Liu, Z. T. Wu, Y. Fan, and E. M. Tentzeris, "A miniaturized CSRR loaded wide-beamwidth circularly polarized implantable antenna for subcutaneous real-time glucose monitoring," *IEEE Antennas and Wireless Propagation Letters*, vol. 16, pp. 577-580, 2017.

[6] M. K. Magill, A. Conway, and W. G. Scanlon, "Tissue-independent implantable antenna for in-body communications at 2.36–2.5 GHz," *IEEE Trans. Antennas and Propagation*, vol. 65, no. 9, pp. 4406-4417, Sept. 2017.

[7] C. M. Lee, T. C. Yo, F. J. Huang, and C. H. Luo, "Bandwidth enhancement of planar inverted-F antenna for implantable biotelemetry," *Microwave and Optical Technology Letters*, vol. 51, no. 3, pp. 749-752, Mar. 2009.

[8] C. L. Tsai, K. W. Chen, and C. L. Yang,, "Implantable wideband low-SAR antenna with c-shaped coupled ground," *IEEE Antennas and Wireless Propagation Letters*, vol. 14, pp. 1594-1597, 2015.

[9] A. C. Durgun, C. A. Balanis, C. R. Birtcher, and D. R. Allee, "Design, simulation, fabrication and testing of flexible bow-tie antennas," *IEEE Trans. Antennas and Propagation*, vol. 59, no. 12, pp. 4425-4435, Dec. 2011.

[10] M. L. Scarpello, D. Kurup, H. Rogier, D. V. Ginste, F. Axisa, J. Vanfleteren, W. Joseph, L. Martens, and G. Vermeeren, "Design of an implantable slot dipole conformal flexible antenna for biomedical applications," *IEEE Trans. Antennas and Propagation*, vol. 59, no. 10, pp. 3556-3564, Oct. 2011.

[11] C. L. Tsai, K. W. Chen, and C. L. Yang, "Implantable wideband low-specific-absorption rate antenna on a thin flexible substrate," *IEEE Antennas and Wireless Propagation Letters*, vol. 15, pp. 1048-1052, 2016.

[12] S. Zhu, S. Almari, A. O. AlAmoudi, and R. J. Langley, "Implanted antenna efficiency improvement," *in Proc. 7th Eur. Conf. Antennas Propagation*, Gothenburg, Sweden, Apr. 2013, pp. 3247-3248.

[13] S. Almari, A. AlAmoudi, and R. J. Langley, "Gain enhancement of implanted antenna using lense and parasitic ring," *Electronics Letters*, vol. 52, no. 10, May 2016.

[14] G. Lovat, P. Burghignoli, F. Capolini, and D. R. Jackson, "Combinations of low/ high permittivity and/or permeability substrates for highly directive planar metamaterial antennas," *IET Microwave Antennas Propagation*, vol. 1, pp. 177-183, 2007.

[15] D. Mitra, A. Sarkhel, O. Kundu, and S. R. B. Chaudhuri, "Design of compact and high directive slot antenna using grounded metamaterial slab," *IEEE Antennas and Wireless Propagation Letters*, vol. 14, pp. 811-814, 2015.

[16] D. Mitra, B. Ghosh, A. Sarkhel, and S. R. B. Chaudhuri, "A miniaturized ring slot antenna design with enhanced radiation characteristics," *IEEE Trans. Antennas and Propagation*, vol. 64, no. 1, pp. 300–305, Jan. 2016.

[17] B. Majumder, K. Krishnamoorthy, J. Mukherjee, and K. P. Ray, "Compact broadband directive slot antenna loaded with cavities and single and double layers of metasurfaces," *IEEE Trans. Antennas and Propagation*, vol. 64, no. 11, pp. 4595-4606, Nov. 2016.

[18] D. Nikolayev, M. Zhadobov, P. karban, and R. Sauleau, "Increasing the radiation efficiency and matching stability of in-body capsule antennas," *in Proc. 10th Eur. Conf. Antennas Propagation*, Davos, Switzerland, Apr. 2016, pp.1-5.

[19] E. Y. Chow, C. Yang, and P. P. Irazoqui, "Wireless powering and propagation of radio frequencies through tissue," in *Wireless Power Transfer*. Aalborg, Denmark: River Publishers, 2012, ch. 9.

[20] D. Schurig, J. J. Mock, and D. R. Smith, "Electric-field-coupled resonators for negative permittivity metamaterials," *Appl. Phys. Lett.*, vol. 88, pp. 041109:1–3, 2006.

[21] Z. Szabó, G. H. Park, R. Hedge, and E. P. Li, "A unique extraction of metamaterial parameters based on Kramers–Kronig relationship," *IEEE Trans. on Microwave Theory and Techniques*, vol. 58, no. 10, pp. 2646-2653, Oct. 2010.

[22] S. A. A. Shah, and H. Yoo, "Scalp-implantable antenna systems for intracranial pressure monitoring," *IEEE Trans. Antennas and Propagation*, vol. 66, no. 4, pp. 2170-2173, Apr. 2018.

[23] N. H. Ramli, M. R. Kamarudin, N. A. Samsuri, E. N. Ahyat, and N. H. H. Khamis, "A 4.8GHz implantable small printed antenna for wireless implantable body area network applications," *in Proc. IEEE International RF and Microwave Conference*, Penang, Malaysia, Dec. 2013, pp. 210-213.

[24] S. Trabelsi, "Variation of the dielectric properties of chicken meat with frequency and temperature," *Journal of Food Measurement and characterization*, vol. 9, pp. 299-304, 2015.